Journal of Power Sources 229 (2013) 42–47

Contents lists available at SciVerse ScienceDirect

Journal of Power Sources

journal homepage: www.elsevier.com/locate/jpowsour

Catalytic activities of PtBi nanoparticles toward methanol electrooxidation in acid and alkaline media

Minli Yang*

General Research Institute for Nonferrous Metals, 2 Xinjiekouwai Street, Beijing 100088, China

HIGHLIGHTS

- ► PtBi nanoparticles are prepared by a simple potentiostatic deposition.
- ► These nanoparticles have a spherical shape and a preset composition.
- ► They have a good catalysis toward methanol electrooxidation in alkaline media.

GRAPHICAL ABSTRACT

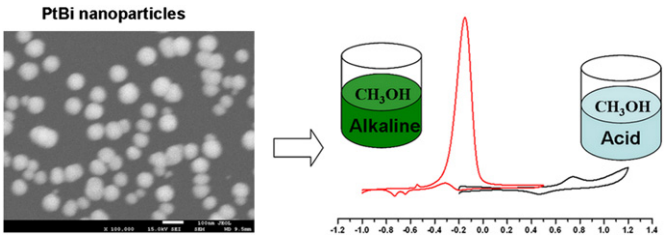

ARTICLE INFO

Article history:
Received 16 August 2012
Received in revised form
13 November 2012
Accepted 30 November 2012
Available online 12 December 2012

Keywords:
Nanoparticles
Catalysis
Electrodeposition
Platinum–bismuth alloy
Methanol
Fuel cells

ABSTRACT

Spherical PtBi nanoparticles are electrodeposited from aqueous solution according to the preset composition. Their catalytic activities toward methanol electrooxidation are examined by cyclic voltammetry and chronoamperometry in acid media and first in alkaline media. Experimental results show that, methanol electrooxidation has lower onset potentials on PtBi than on Pt in either acid or alkaline media. The improved catalytic activities are due to the electronic effects of bismuth in PtBi. At higher overpotentials, the electrolyte acidity has produced different influences on the kinetics of methanol electrooxidation on PtBi and Pt. In acid media, PtBi is inferior to Pt for methanol oxidation at above 0.460 V, because that fewer continuous Pt sites on PtBi are not enough for the adsorption and dehydrogenation of methanol molecules. In alkaline media, the oxidation current on PtBi becomes much higher than that on Pt at above 0.768 V. The raised current can be credited to the bifunctional mechanism. Bi_2O_5 sites on PtBi surface serve for OH_{ad} adsorption and Pt sites for methanol dehydrogenation. The better catalytic activity of PtBi nanoparticles in alkaline media suggests their promising application in alkaline direct alcohol fuel cells.

1. Introduction

As a model reaction, the electrocatalytic oxidation of methanol has been attracting much interest in the last four decades. Early works proved that, platinum can promote the methanol dehydrogenation effectively, but the CO molecules adsorbed at Pt surface may block the active sites. To decrease CO poisoning, many researchers have turned to exploring multimetallic catalysts and got some promising results. The improved catalytic activities have been explained according to bifunctional mechanism [1], electronic effects [2,3], or ensemble effects [4]. Besides the most intensively researched PtRu alloy, PtBi bimetallic catalysts have also received much attention for the electrooxidation of small organic molecules including methanol.

Recently, Abruna and co-workers [5–9] explored the PtBi intermetallic compounds for the catalytic oxidation of CO and some small organic molecules. These authors concluded that, although the PtBi intermetallic phases present virtual immunity to CO poisoning and have an improved activity toward formic acid and formaldehyde oxidation, they are inactive to methanol

* Tel./fax: +86 10 62013148.
E-mail address: myangbjcn@gmail.com.

0378-7753/$ – see front matter © 2012 Elsevier B.V. All rights reserved.
http://dx.doi.org/10.1016/j.jpowsour.2012.11.150

electrooxidation. Such an opinion also appeared in the study by Jeyabharathi et al. [10]. However, the work by Du and Wang [11] displayed that bismuth modified Pt nanoparticles/indium tin oxide (PtNPs/ITO) has higher activity and better stability than the PtNPs/ITO. Li et al. [12] also demonstrated that PtBi/XC-72 is more active toward methanol oxidation and has better CO tolerance than PtRu/C. Since the different conclusions may be related to the catalyst preparation and the influence of supports, it is necessary to reexamine the catalytic performance of PtBi with a simpler preparation.

As for the PtBi alloy preparation, several methods have been reported, such as induction melting [13], "water-in-oil" microemulsion method [14], polyol process [6,10], reduction by sodium borohydride [15,16] and sodium hypophosphite [12], solution chemistry method [17], and H_2/N_2 reduction [18]. To our knowledge, however, there has been no publication about the direct electrodeposition of PtBi nanoparticles. As an easy and reproducible process, electrodeposition has been considered a convenient technique to prepare metal and alloy catalysts for direct alcohol fuel cells [19,20].

In addition, up to now, there are few publications on methanol electrooxidation at PtBi in alkaline media. Matsumoto [21] studied the electrocatalytic activities of PtBi and $PtBi_2$ intermetallic compounds toward methanol oxidation in 0.1 M KOH solution, reaching a conclusion that PtBi and $PtBi_2$ had high catalytic activities in alkaline solutions. Also, some recent studies involving other catalysts [22–27] have demonstrated that alkaline solution can make the methanol electrooxidation occur at less positive potentials. We believe that the information obtained in highly alkaline media will also deepen the understanding of PtBi catalyst. Therefore, in this paper, we present and explain the results obtained with PtBi nanoparticles and Pt nanoparticles in 0.5 M H_2SO_4 and 1.0 M NaOH solutions.

2. Experimental

All chemicals used were of analytical grade. Chloroplatinic acid and ruthenium chloride were bought from Sino-Platinum Co., Ltd. (Kunming, China). Other chemicals were purchased from Beijing Chemical Reagents Company. All solutions were prepared with deionized water.

Electrochemical experiments were performed with a CHI630D electrochemical analyzer (CH Instruments, Shanghai). Glassy carbon electrodes (GCEs) served as the working electrodes, with the Ag/AgCl (saturated KCl) electrode and platinum wire as the reference and counter electrode, respectively. All potentials were referred to the reversible hydrogen electrode (RHE). The current was normalized by the Pt mass, which was determined according to the total charge during electrodeposition and the Pt content.

Prior to each experiment, the electrolyte was deaerated with pure N_2 for 15 min. GCEs were hand-polished with alumina slurries (0.3 μm and then 0.05 μm), followed by the sonication in ethanol and deionized water. The Pt and PtBi nanoparticles were electrodeposited at −0.15 V vs. Ag/AgCl for 300 s from the 0.5 M H_2SO_4 solutions of 1 mM $[PtCl_6]^{2-}$ ions and 1 mM $[PtCl_6]^{2-}$ + 0.9 mM Bi^{3+} ions, respectively. The determination of deposition potential was based on the CVs of the mixed electrolyte of $[PtCl_6]^{2-}$ and Bi^{3+} ions.

After being rinsed with deionized water and dried under a stream of N_2, the resultant products were immediately characterized with X-ray diffraction (XRD) (Philips X'Pert MRD), X-ray spectroscopy (EDX) and Scanning electron microscopy (*SEM*) (JEOL JSM-7001F). The cyclic voltammetry (CV) tests of methanol electrooxidation were carried out within a potential scope from zero to 1.2 V vs. Ag/AgCl (acid media) and within a potential scope from −1.0 to 0.5 V vs. Ag/AgCl (alkaline media), at a scan rate of 50 mV s^{-1}. The chronoamperometry (CA) responses were recorded at 0.5 V vs. Ag/AgCl for 1200 s (acid media) and at −0.3 V vs. Ag/AgCl for 1200 s (alkaline media). To get the Tafel plots, we performed quasi-steady-state voltammetry measurements at 10 mV s^{-1}.

3. Results and discussion

3.1. Characterizations of electrodeposited PtBi nanoparticles

The co-deposition of Pt and Bi was studied by the CVs of the mixed electrolyte of $[PtCl_6]^{2-}$ and Bi^{3+} ions. Fig. 1 shows the comparative CVs recorded at the first potential cycles. In the CV of 1 mM H_2PtCl_6 solution, there is a sharp increase in reduction current when the forward scan is over 0.0 V, which resulted from the hydrogen evolution at Pt deposit. The current peaks marked with a and a' were attributed to the reduction of Pt^{4+} into Pt^0, while peaks b and c corresponded to the redox of Bi^{3+}/Bi^0. Since the oxidation peak of pure bismuth usually occurs at a potential about 0.2 V vs. Ag/AgCl [28,29], the dramatic shift of peak c in anodic direction (see Fig. 1) may be due to a significant free energy change or some kinetic factor [30], suggesting the formation of PtBi alloys. Based on the CV results, we selected −0.15 V vs. Ag/AgCl as the deposition potential, with an assumption that deposit compositions rely on the bath electrolyte under diffusion control.

Fig. 2 displays the XRD characterizations of as-prepared Pt/Bi codeposit and background electrode. In the XRD pattern of background electrode, most of the sharp peaks match well with polytetrafluorethylene (PTFE) (JCPDS 47-2217), and the broad peaks at about 25.5° and 78.8° probably result from glassy carbon. In the XRD pattern of sample electrode, the four new peaks signed by dotted lines are consistent with those reported in literature, whose appearance was considered an indication of PtBi alloy phase [15,16].

The morphology and chemical composition of PtBi product were determined by the SEM and EDX characterizations. Fig. 3 shows that spherical PtBi nanoparticles cover the electrode surface uniformly. The analysis result by image software indicated that the average size of PtBi nanoparticles was 63 ± 20 nm in diameter. The EDX spectrum in Fig. 3 displays the presence of C, O, Pt, and Bi. The carbon signal resulted from the GCE, and the oxygen signal could be ascribed to the partial oxidation of bismuth in air [15,31]. The measured atomic ratio of Pt to Bi (1.18) is close to the molar ratio of $[PtCl_6]^{2-}$ to Bi^{3+} ions in electrolyte (1.11).

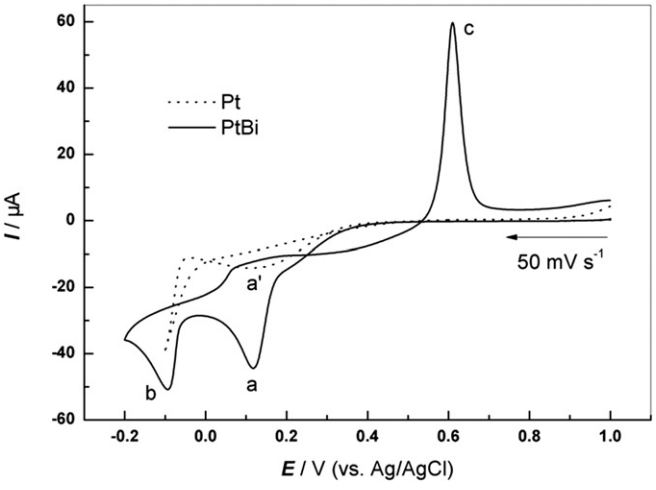

Fig. 1. Cyclic voltammograms for 1 mM H_2PtCl_6 (dotted line), and 1 mM H_2PtCl_6 + 0.9 mM $Bi(NO_3)_3$ (solid line), in 0.5 M H_2SO_4.

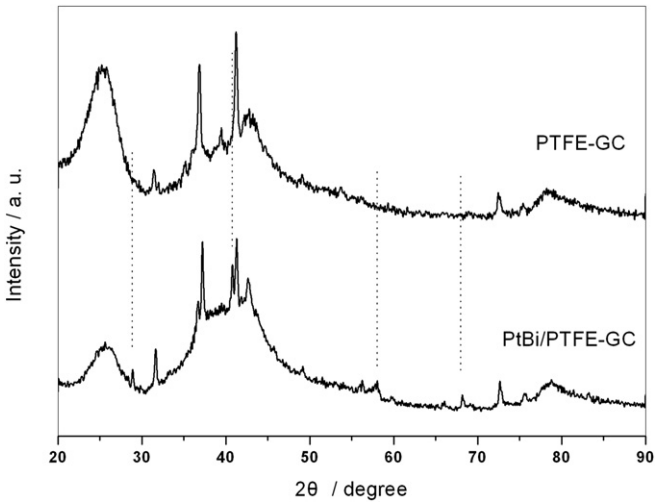

Fig. 2. XRD pattern of the PtBi electrodeposit at PTFE-shrouded GCEs. PTFE: polytetrafluorethylene.

3.2. Methanol electrooxidation on PtBi nanoparticles

The catalytic activities of PtBi nanoparticles toward methanol electrooxidation were investigated with CV and CA in acid and alkaline media, respectively. For comparison, Pt nanoparticles were also prepared and used for methanol electrooxidation under the same conditions. Considering the difficulty in measuring the specific surface area of the nanoparticles adhered to electrode surfaces [15], we compared the two nanoparticle catalysts with each another by the Pt mass-specific activity in this work.

Fig. 4 shows the CV curves and their local magnification for methanol electrooxidation in 0.5 M H_2SO_4 solution. The most obvious difference is embodied in the forward anodic peaks (Fig. 4a). The peak potential for Pt nanoparticles ($E_{p,\ Pt}$) is less positive than that for PtBi nanoparticles ($E_{p,\ PtBi}$), and the peak currents show a sequence of $I_{p,\ Pt} > I_{p,\ PtBi}$. These results verify that, from the viewpoint of kinetics, Pt nanoparticles have much better catalytic activity than the PtBi nanoparticles. However, the local magnifications (Fig. 4b) revealed that, the onset potential for methanol oxidation at PtBi nanoparticles is about 25 mV less positive than that at Pt nanoparticles. In fact, such a potential difference existed also in the experimental results by Abruna group [15]. Fig. 5 shows the CA responses recorded at 0.5 V vs. Ag/AgCl for Pt and PtBi modified GCEs. During the whole run time, the methanol electrooxidation catalyzed by PtBi nanoparticles produced the lower current. Quantitatively, at the end of CA measurement, the current at Pt nanoparticles was 11 times higher than that at PtBi nanoparticles. These CV and CA results demonstrated that, in spite of the slight thermodynamic advantage, the kinetic activity of PtBi nanoparticles for methanol oxidation was inferior to that of Pt nanoparticles in acid media.

Figs. 6 and 7 report the CV and CA responses recorded in alkaline media. First, the methanol oxidation is faster in alkaline media than in acid media. According to the explanation by Tripkovic and coworkers [32], the absence of bisulfate anions is beneficial to the access of methanol molecules or OH_{ad} to Pt sites. The most impressive features are the current peaks in CV responses. The peak potential $E_{p,\ PtBi}$ is more positive than $E_{p,\ Pt}$, but the peak current $I_{p,\ PtBi}$ is much larger than $I_{p,\ Pt}$. The onset potential at PtBi nanoparticles becomes about 125 mV less positive than that at Pt nanoparticles (Fig. 6b). In Fig. 7, at the end of CA measurement, the current of methanol oxidation at PtBi is about 19 times higher than that at Pt. The much-enhanced peak current at PtBi nanoparticles resulted from the influence of electrolyte on the surface state of catalyst, which will be discussed in the following section.

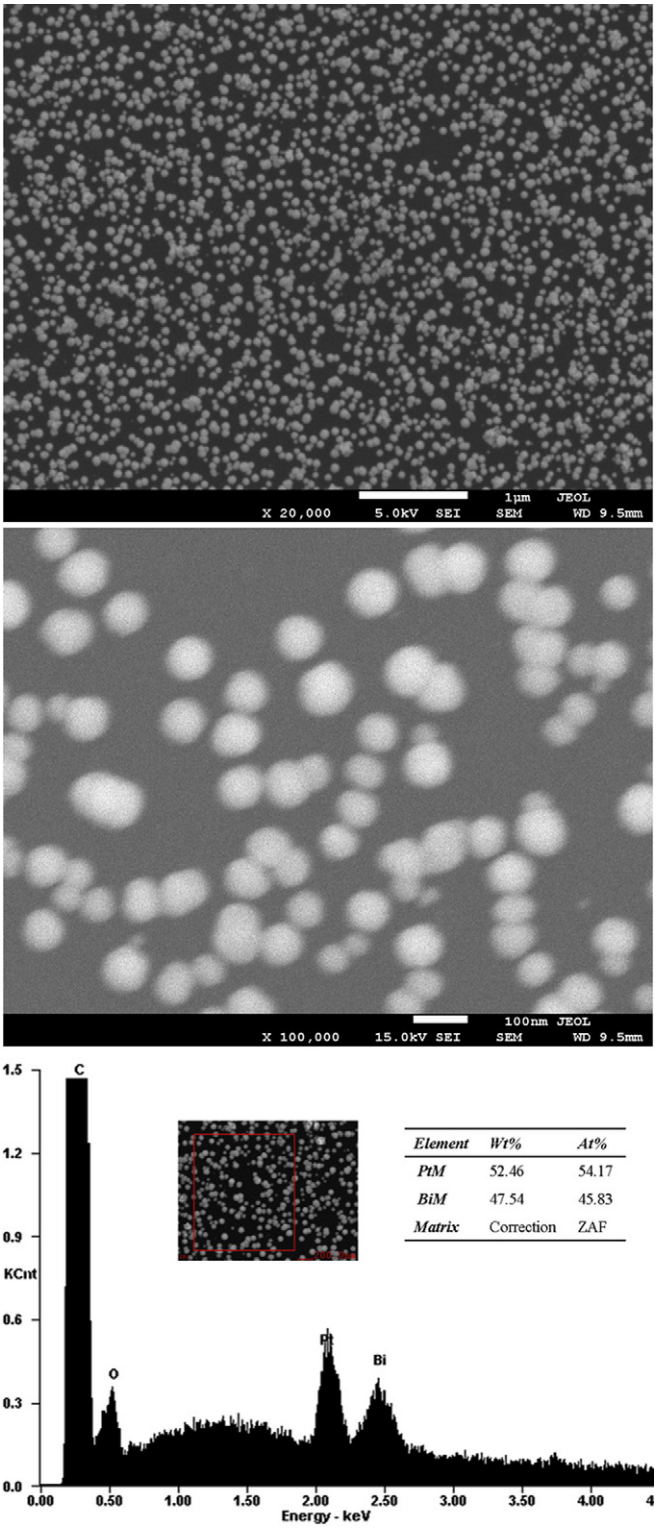

Fig. 3. SEM micrographs at different magnifications (upper, middle) and EDX spectrum (bottom) of PtBi electrodeposit. The insets of EDX spectrum are the corresponding sampling region and quantitative analysis, respectively.

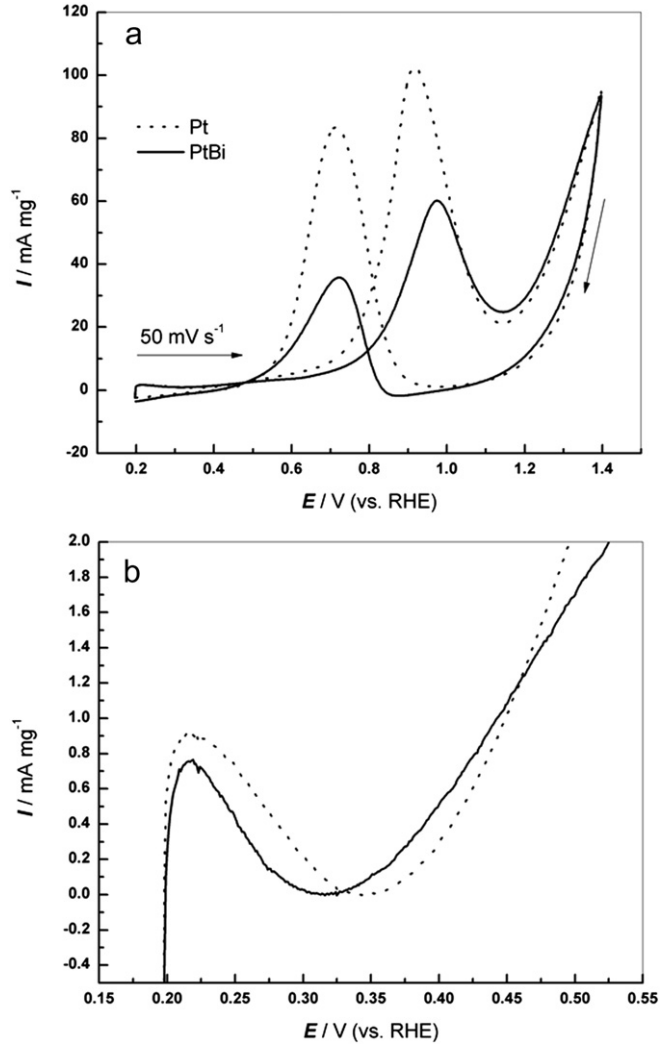

Fig. 4. Cyclic voltammograms (a) and their local magnification (b) for 1.0 M CH_3OH + 0.5 M H_2SO_4 at GCEs covered with Pt and PtBi nanoparticles, respectively.

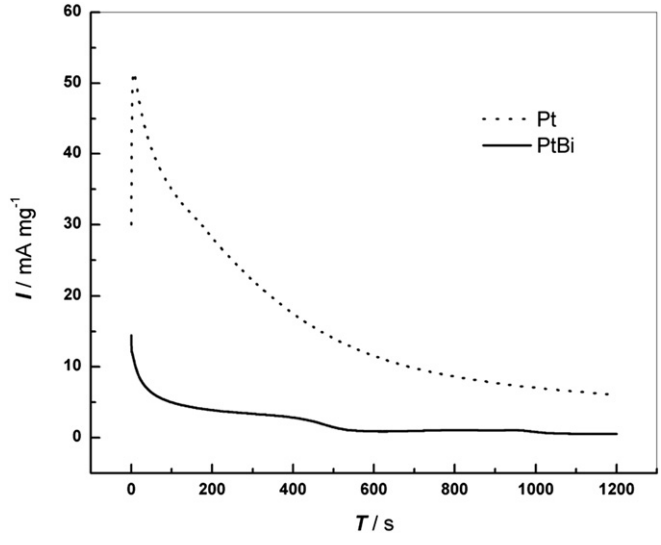

Fig. 5. Chronoamperometric curves for 1.0 M CH_3OH + 0.5 M H_2SO_4 at GCEs covered with Pt and PtBi nanoparticles, respectively. At 0.5 V vs. Ag/AgCl for 1200 s.

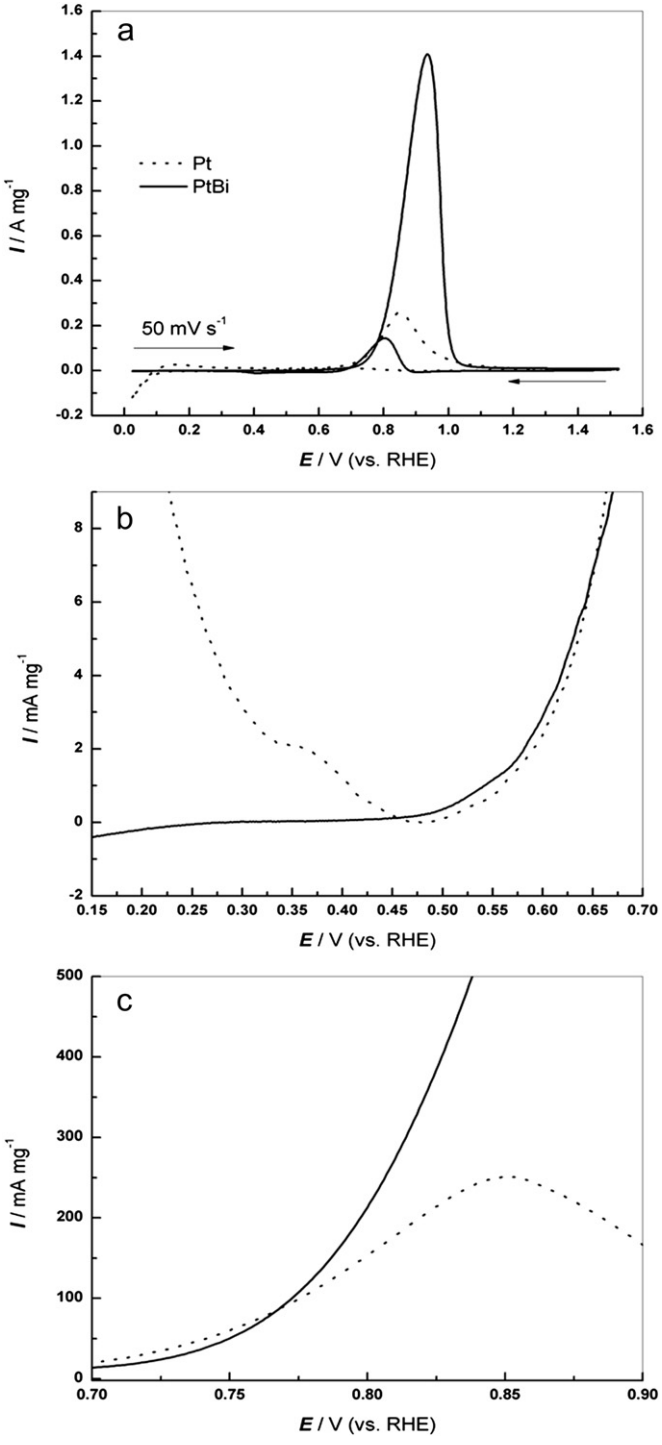

Fig. 6. Cyclic voltammograms (a) and their local magnification (b, c) for 1.0 M CH_3OH + 1.0 M NaOH at GCEs covered with Pt and PtBi nanoparticles, respectively.

3.3. Roles of bismuth species in PtBi nanoparticle catalyst

To explore the chemical states of bismuth species in PtBi, we checked the multicycle background CVs of PtBi nanoparticle electrode in acid and alkaline media. The CV features in H_2SO_4 (Fig. 8) are much similar to those reported by Daniele and Bergamin [33] and those by Lee et al. [34]. We preferred to assign the three anodic peaks (peaks a, b and c) to the stepwise formation of adsorbed $Bi(OH)_2$, soluble $Bi(OH)_2^+/Bi(OH)^{2+}$, and Bi^{3+}, respectively.

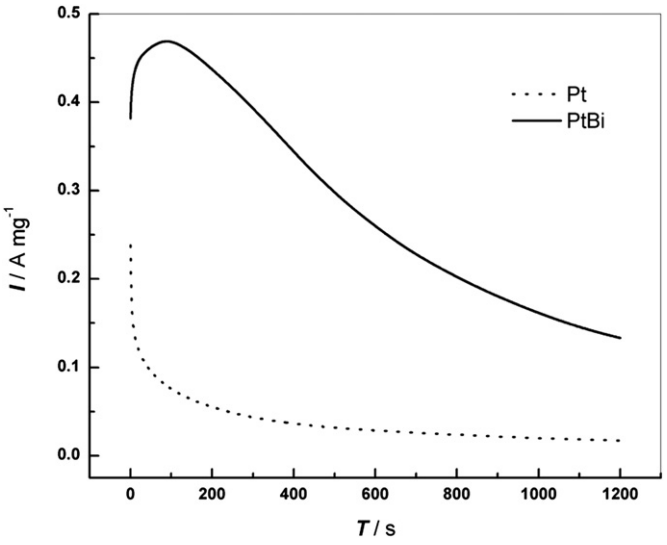

Fig. 7. Chronoamperometric curves for 1.0 M CH_3OH + 1.0 M NaOH at GCEs covered with Pt and PtBi nanoparticles, respectively. At −0.3 V vs. Ag/AgCl for 1200 s.

Also, the changes of peaks c and *d* are similar to those reported by Abruna and co-workers [7], suggesting the gradual leaching of bismuth from PtBi alloy.

The CV responses in NaOH (Fig. 8) resemble those in the papers by Demarconnay and coworkers [14,35], where these authors implied that bismuth was difficult to leach from the catalyst surface in alkaline media. Based on the present work and those in literature, the peaks a' and b' could be ascribed to the formation of Bi_2O_3 and Bi_2O_5, respectively. The peak c' corresponded to the reduction of Bi_2O_5, while the peak d' was related to the reduction of Bi_2O_3 to Bi. The different chemical states of bismuth species could be responsible for the catalytic performances of PtBi nanoparticles in acid and alkaline media.

As shown above, with PtBi nanoparticles as catalyst, the methanol electrooxidation has a less positive onset potential and slightly higher current until 0.460 V in acid media. Since the potential of 0.460 V is far from the three anodic peaks for bismuth in H_2SO_4 (Fig. 8), the bifunctional catalysis [11,12] is likely impossible, at least under the conditions of our experiment. The possible reason for the catalytic ability is the electronic effect [16,36,37]. The Bi atoms could improve the OH_{ad} adsorption on the Pt sites [36], and could reduce the inclination for CO adsorption on PtBi surfaces through raising the Fermi level of the system [37].

Above 0.460 V, since the Pt sites were enough active for the OH_{ad} adsorption, the adsorption and dehydrogenation of methanol molecules would become the rate-limiting step gradually. In our quasi-steady-state voltammetry experiments (Fig. 9), the linear portions of the Tafel plots were fitted linearly. The coefficients of determination (R^2) are 0.992 for the plot corresponding to 0.5 M H_2SO_4 solution and 0.990 for that corresponding to 1.0 M NaOH solution. The Tafel slope values are 113 mV dec^{-1} for 0.5 M H_2SO_4 solution and 56 mV dec^{-1} for 1.0 M NaOH solution. A Tafel slope value close to 120 mV dec^{-1} often suggests that the adsorption and dehydrogenation of methanol molecules is the rate-limiting step [38,39]. As known, bismuth is not a good catalyst like Pt for the adsorption and dehydrogenation of methanol molecules. Even though some bismuth atoms leached from PtBi alloy at more positive potentials, the resulted discontinuous Pt sites could not provide intermediate CO_{ad} as quick as the Pt nanoparticles. As a result, at potentials more positive than 0.460 V, PtBi nanoparticles

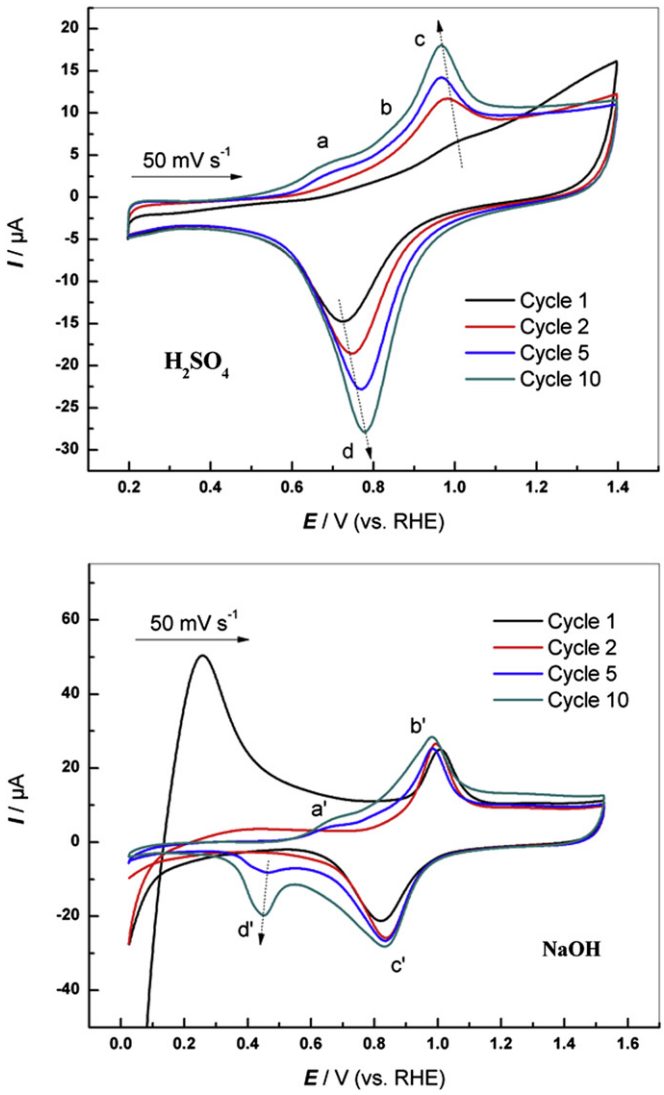

Fig. 8. Multicycle cyclic voltammograms for the PtBi nanoparticle covered GCE in 0.5 M H_2SO_4 (upper) and 1.0 M NaOH (lower).

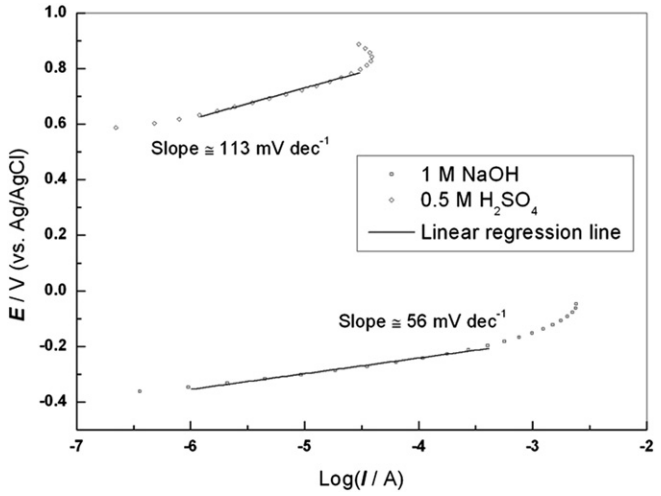

Fig. 9. Tafel plots for the electrooxidation of 1.0 M CH_3OH at PtBi/GCE in 1.0 M H_2SO_4 and 0.5 M NaOH solutions, respectively.

had a worse performance than Pt nanoparticles for methanol oxidation in acid media.

As for the methanol electrooxidation in alkaline media, there are two opinions: the formate path [40–42] and the CO path [32,43]. Recently, Spendelow et al. [39] pointed out that, methanol oxidation occurs through a CO intermediate at below 0.45 V and the CO-to-carbonate pathway shifts to the formate pathway at potentials higher than 0.5 V. In contrary, Matsuoka et al. [44] demonstrated that, methanol oxidation proceeds mainly in the methanol-reactive intermediate-formate path at 0.4 V and the CO-to-carbonate pathway becomes more significant with increasing potential. Considering the onset potentials in our experiment (0.35 V for PtBi and 0.475 V for Pt) and the similarity between our working electrodes and platinized Pt, we preferred to discuss our experimental results with the mechanism by Matsuoka et al. [44]. This is partly supported by the Tafel slope value of 56 mV dec^{-1} for NaOH solution (Fig. 9), which is much close to the theoretical value of 60 mV dec^{-1} for Langmuir–Hinshelwood CO oxidation.

In alkaline media, the less positive onset potential and the slightly higher current until 0.640 V probably also resulted from the electronic effect. At above 0.768 V (Fig. 6c), the oxidation current on PtBi became higher again than that on Pt and had a rapid increase. Since the value of 0.768 V is between the potentials for peaks a' (Bi_2O_3) and b' (Bi_2O_5) in Fig. 8, the much higher current is probably due to the Bi_2O_5 formation. It is supposed that, Bi_2O_5 could serve as the sites for OH_{ad} adsorption and Pt sites could be available for methanol dehydrogenation, making the bifunctional mechanism take effects.

4. Conclusions

Spherical PtBi nanoparticles with the preset composition have been produced by a simple potentiostatic deposition. The catalysis performances of PtBi nanoparticles toward methanol electrooxidation have been explored in acid and alkaline media. Experimental results demonstrate that, at low overpotentials, PtBi nanoparticles have better catalytic activity toward methanol electrooxidation than Pt nanoparticles in either acid or alkaline media. The improved catalytic activities are due to the electronic effects of bismuth in PtBi.

The influences of electrolyte acidity are embodied mainly in the kinetic aspect of methanol electrooxidation at PtBi nanoparticles. In acid media, PtBi is inferior to Pt for methanol oxidation at above 0.460 V. The reason is probably that fewer continuous Pt sites on PtBi are not enough for the adsorption and dehydrogenation of methanol molecules. In alkaline media, however, the oxidation current on PtBi becomes much higher than that on Pt at above 0.768 V. The enhanced current can be attributed to the effect of Bi_2O_5 on PtBi surface. Bi_2O_5 can serve as the sites for OH_{ad} adsorption, and Pt sites are available for methanol dehydrogenation, making the bifunctional mechanism take effects.

Either in thermodynamics or in kinetics, PtBi nanoparticles show a better catalytic activity toward methanol oxidation than Pt nanoparticles in alkaline media, suggesting the promising application of PtBi nanoparticles in alkaline direct alcohol fuel cells.

Acknowledgments

Thank the financial support by National Natural Science Foundation of China (Grant No. 50871024).

References

[1] M. Watanabe, S. Motoo, J. Electroanal. Chem. 60 (1975) 267–273.
[2] P. Waszczuk, J. Solla-Gullón, H.S. Kim, Y.Y. Tong, V. Montiel, A. Aldaz, A. Wieckowski, J. Catal. 203 (2001) 1–6.
[3] T. Bligaard, J.K. Nørskov, Electrochim. Acta 52 (2007) 5512–5516.
[4] V. Climent, N. Garcia-Araez, J.M. Feliu, in: M.T.M. Koper (Ed.), Fuel Cell Catalysis: A Surface Science Approach, John Wiley & Sons, Inc., Hoboken, New Jersey, 2009.
[5] E. Casado-Rivera, D.J. Volpe, L. Alden, C. Lind, C. Downie, T. Vázquez-Alvarez, A.C.D. Angelo, F.J. DiSalvo, H.D. Abruña, J. Am. Chem. Soc. 126 (2004) 4043–4049.
[6] C. Roychowdhury, F. Matsumoto, P.F. Mutolo, H.D. Abruña, F.J. DiSalvo, Chem. Mater. 17 (2005) 5871–5876.
[7] D.R. Blasini, D. Rochefort, E. Fachini, L.R. Alden, F.J. DiSalvo, C.R. Cabrera, H.D. Abruna, Surf. Sci. 600 (2006) 2670–2680.
[8] H.S. Wang, L. Alden, F.J. DiSalvo, H.D. Abruna, Phys. Chem. Chem. Phys. 10 (2008) 3739–3751.
[9] N. de-los-Santos-Alvarez, L.R. Alden, E. Rus, H. Wang, F.J. DiSalvo, H.D. Abruna, J. Electroanal. Chem. 626 (2009) 14–22.
[10] C. Jeyabharathi, J. Mathiyarasu, K. Phani, J. Appl. Electrochem. 39 (2009) 45–53.
[11] Y. Du, C. Wang, Mater. Chem. Phys. 113 (2009) 927–932.
[12] X. Li, G. Chen, J. Xie, L.J. Zhang, D.G. Xia, Z.Y. Wu, J. Electrochem. Soc. 157 (2010) B580–B584.
[13] A.V. Tripkovic, K.D. Popovic, R.M. Stevanovic, R. Socha, A. Kowal, Electrochem. Commun. 8 (2006) 1492–1498.
[14] L. Demarconnay, S. Brimaud, C. Coutanceau, J.M. Leger, J. Electroanal. Chem. 601 (2007) 169–180.
[15] C. Roychowdhury, F. Matsumoto, V.B. Zeldovich, S.C. Warren, P.F. Mutolo, M. Ballesteros, U. Wiesner, H.D. Abruna, F.J. DiSalvo, Chem. Mater. 18 (2006) 3365–3372.
[16] M.M. Tusi, N.S.O. Polanco, S.G. da Silva, E.V. Spinacé, A.O. Neto, Electrochem. Commun. 13 (2011) 143–146.
[17] J.C. Bauer, X. Chen, Q.S. Liu, T.H. Phan, R.E. Schaak, J. Mater. Chem. 18 (2008) 275–282.
[18] X.L. Ji, K.T. Lee, R. Holden, L. Zhang, J.J. Zhang, G.A. Botton, M. Couillard, L.F. Nazar, Nat. Chem. 2 (2010) 286–293.
[19] A. Lima, C. Coutanceau, J.M. Leger, C. Lamy, J. Appl. Electrochem. 31 (2001) 379–386.
[20] C. Coutanceau, S. Brimaud, C. Lamy, J. Leger, L. Dubau, S. Rousseau, F. Vigier, Electrochim. Acta 53 (2008) 6865–6880.
[21] F. Matsumoto, Electrochemistry 80 (2012) 132–138.
[22] L.X. Yang, W.Y. Yang, Q.Y. Cai, J. Phys. Chem. C 111 (2007) 16613–16617.
[23] C.W. Xu, L.Q. Cheng, P.K. Shen, Y.L. Liu, Electrochem. Commun. 9 (2007) 997–1001.
[24] E.E. Switzer, T.S. Olson, A.K. Datye, P. Atanassov, M.R. Hibbs, C.J. Cornelius, Electrochim. Acta 54 (2009) 989–995.
[25] X.Z. Fu, Y. Liang, S.P. Chen, J.D. Lin, D.W. Liao, Catal. Commun. 10 (2009) 1893–1897.
[26] W.Q. Zhou, C.Y. Zhai, Y.K. Du, J.K. Xu, P. Yang, Int. J. Hydrogen Energy 34 (2009) 9316–9323.
[27] Q.A. Jiang, L.H. Jiang, S.L. Wang, J. Qi, G.Q. Sun, Catal. Commun. 12 (2010) 67–70.
[28] M. Yang, Z. Hu, J. Electroanal. Chem. 583 (2005) 46–55.
[29] M. Yang, J. Mater. Chem. 21 (2011) 3119–3124.
[30] V.D. Jović, R.M. Zejnilović, A.R. Despić, J.S. Stevanović, J. Appl. Electrochem. 18 (1988) 511–520.
[31] S. Derrouiche, C.Z. Loebick, L. Pfefferle, J. Phys. Chem. C 114 (2010) 3431–3440.
[32] A.V. Tripkovic, K.D. Popovic, B.N. Grgur, B. Blizanac, P.N. Ross, N.M. Markovic, Electrochim. Acta 47 (2002) 3707–3714.
[33] S. Daniele, S. Bergamin, Electrochem. Commun. 9 (2007) 1388–1393.
[34] J. Lee, P. Strasser, M. Eiswirth, G. Ertl, Electrochim. Acta 47 (2001) 501–508.
[35] L. Demarconnay, C. Coutanceau, J.M. Leger, Electrochim. Acta 53 (2008) 3232–3241.
[36] T.J. Schmidt, R.J. Behm, B.N. Grgur, N.M. Markovic, P.N. Ross, Langmuir 16 (2000) 8159–8166.
[37] M. Oana, R. Hoffmann, H.D. Abruña, F.J. DiSalvo, Surf. Sci. 574 (2005) 1–16.
[38] T.H.M. Housmans, M.T.M. Koper, J. Phys. Chem. B 107 (2003) 8557–8567.
[39] J.S. Spendelow, J.D. Goodpaster, P.J.A. Kenis, A. Wieckowski, Langmuir 22 (2006) 10457–10464.
[40] W. Vielstich, Fuel Cells, Wiley Interscience, London, 1970.
[41] A.V. Tripkovic, K.D. Popovic, J.D. Lovic, V.M. Jovanovic, A. Kowal, J. Electroanal. Chem. 572 (2004) 119–128.
[42] P.A. Christensen, D. Linares-Moya, J. Phys. Chem. C 114 (2010) 1094–1101.
[43] E. Morallón, A. Rodes, J.L. Vázquez, J.M. Pérez, J. Electroanal. Chem. 391 (1995) 149–157.
[44] K. Matsuoka, Y. Iriyama, T. Abe, M. Matsuoka, Z. Ogumi, Electrochim. Acta 51 (2005) 1085–1090.